ARTICLES

Mechanical Activation of Structural and Chemical Transformations in a Zr−C−H System in Two Stages

C. Borchers,*,† A. V. Leonov,‡ and O. S. Morozova§

Institute of Materials Physics, University of Göttingen, Hospitalstrasse 3-7, 37073 Göttingen, Germany, Chemical Department, M. V. Lomonosov Moscow State University, Leninskie Gory, 119899 Moscow, Russia, and N. N. Semonov Institute of Chemical Physics, Kosygin Str. 4, 117334 Moscow, Russia

Received: July 5, 2001; In Final Form: October 15, 2001

The effect of mechanical activation on the structural and chemical transformations in the zirconium−carbon−hydrogen system was studied using X-ray powder diffraction, transmission electron microscopy and kinetic techniques. A zirconium−graphite mixture was subjected to high-energy impact milling in a permanent hydrogen flow. A two-stage process was observed: first, the formation of tetragonal ϵ-$ZrH_{1.8-2}$ accompanied by carbon amorphization, and second the decomposition of ϵ-$ZrH_{1.8-2}$ synthesized at the first stage to cubic δ-$ZrH_{1.6}$ + γ-ZrH + α-Zr. In the first stage, the size of the hydride particles decreased drastically to only a few nanometers dispersed in larger particles of amorphous carbon, while in the second stage the newly formed Zr particles compacted again to gain the size of microns, while the carbon partially crystallized. While the first stage is governed by the fast reaction kinetics of hydrogen with zirconium, the second stage is governed by the greater affinity of zirconium to carbon as compared to hydrogen.

1. Introduction

According to recent publications, it is feasible to apply high-energy impact milling as a promising technique for fast and low cost synthesis of widely used materials: metallic hydrides, nitrides, and carbides from elements at room temperature.[1−3] The mechanical treatment of a zirconium−graphite mixture results in the formation of a highly dispersed amorphous or cubic ZrC phase.[4] Milling of Zr powder under hydrogen in static or flow conditions produces a highly dispersed tetragonal $ZrH_{1.8-2}$ phase,[5] which can be used for hydrogen storage or as a catalyst. Zirconium dihydride loses part of its bulk hydrogen, when milled with graphite in He, CO or CO_2 flow[6] and partly transforms to a cubic ZrH_xC_{1-x} phase under milling conditions.[7] Hydrogen substitution and CH_4 formation accompanied the interaction of ZrH_2 with graphite.[7]

The binary Zr−H and Zr−C systems are well studied.[8−10] It is known that hydrogen atoms are located in the tetrahedral sites of the Zr lattice, whereas larger interstitial impurities, such as C and O atoms, are located in the octahedral sites. The behavior of the ternary Zr−C−H system is poorly known, in particular under mechanical treatment.

It is the aim of this work to compare the reactivity of hydrogen and carbon when both simultaneously react with zirconium under milling conditions, i.e., to investigate the interdependence between the gas−solid and solid−solid reactions mechanically induced. Both the interaction between components in the zirconium−graphite−hydrogen system and the evolution in the microstructure of solids mechanically activated are studied.

2. Experimental

Mechanical activation was carried out in a flow mechanochemical reactor fixed to a vibrator with vibration frequency of 50 Hz and an amplitude of milling of 7.25 mm; the average energy intensity was 1.0 W/g. A stainless steel container was loaded with 1.8 g of Zr, graphite, or reaction mixture (1.5 g Zr + 0.3 g graphite) together with 19.8 g of hardened steel balls (diameter 3−5 mm). The input of the reactor was connected to a setup for preparing gas mixtures; the outlet was combined on-line with a gas chromatograph to analyze the effluent gases. The gas flow rate (∼0.01 L/min) was measured before and after the reactor. The flow mechanochemical reactor and the treatment procedure were described in detail by Streletskii and co-workers.[11] Possible Fe contamination from the cell and balls was checked with a Cameca MBX-1 microprobe in the regime of X-ray analysis. No contamination was found, which is not surprising, since graphite works as a lubricant and the average intensity of the milling process is comparatively low.

The milling was started when the gas concentration at both the input and the outlet of the reactor was equal. The duration of each run ranged from 15 to 190 min. To study the dynamics of the process, the effluent gases were analyzed every 10−20 min. All the experiments were carried out at room temperature and atmospheric pressure. Zirconium powder (99%, H content 3−5%, average particle size ∼50 μm) and graphite (chemically

* Corresponding author. Tel.: 49-551-395584. E-mail: chris@umpa03.gwdg.de.
† University of Göttingen.
‡ M. V. Lomonosov Moscow State University.
§ N. N. Semonov Institute of Chemical Physics.

10.1021/jp0125505 CCC: $22.00
Published on Web 01/31/2002

TABLE 1: Phase Compositions, Zr Content, and the Surface Area of the Samples Milled under Different Conditions

sample	milling time, min	gas	phase composition	Zr content, at. %	surface area, m^2/g
Zr	15	H_2	α-Zr ϵ-$ZrH_{1.8-2}$	~50	0.4
C	120	H_2	C		175
α-Zr + C	120	He	α-Zr + C ZrC	~25	8
α-Zr + C	15	H_2	α-Zr + C ϵ-$ZrH_{1.8-2}$	~20	8.7
α-Zr + C	60	H_2	C ϵ-$ZrH_{1.8-2}$	~2	25
α-Zr + C	85	H_2	ϵ-$ZrH_{1.8-2}$	0	58.4
α-Zr + C	110	H_2	α-Zr + C γ-ZrH δ-$Zr_{1.6}$ ϵ-$ZrH_{1.8-2}$	~20	1.85
α-Zr + C	190	H_2	α-Zr + C γ-ZrH δ-$Zr_{1.6}$ ϵ-$ZrH_{1.8-2}$	~80	<0.3

pure, specific surface area 2 m^2/g) were used as received. From previous experiments it is known that a small part of the carbon reacts with hydrogen to form CH_4. To make sure that all of the Zr will react with carbon to form ZrC, a Zr:C molar ratio of 1:1.45 was used.

Hydrogen sorption on graphite was determined with a gas cromatograph by measuring the hydrogen contents in the input and outlet gas flows. The specific surface area *S* of the powders was measured by the Brunauer−Emmett−Teller (BET)[12] method with low-temperature Ar adsorption. X-ray diffraction (XRD) patterns of the solids were recorded before and after the treatments using a Dron-3 diffractometer with a Cu−Kα anode. The solid phases were identified with the help of the JCPDS file provided by the International Center for Diffraction Data. The Zr content in the powders after mechanical activation was estimated by temperature-programmed reaction with hydrogen (TPR).[13] The TPR measurements for H_2 were carried out at a heating rate of 12°/min from 20 to 550 °C under flow conditions (flow rate 0.1 L/min.) using a H_2/Ar mixture containing 7 vol % of H_2. The microstructure of the powders was studied by scanning electron microscopy (SEM) and transmission electron microscopy (TEM). For SEM, a Cameca MBX-1 microprobe in a regime of scanning microscopy was used. TEM was performed with a Philips EM 420 ST (resolution limit 0.3 nm, information limit 0.2 nm, accelerating voltage 120 kV). For TEM samples, the powder was prepared from an ethanol suspension and placed on copper grids covered by amorphous carbon.

As preliminary experiments, Zr only and graphite only were milled in hydrogen flow; additionally, a mixture of Zr and graphite was milled in He flow. The reaction mixture Zr + graphite was treated for various milling times ranging between 15 and 190 min. The phase composition, Zr content, and the specific surface area of the milling products were determined. The microstructure of the mixed powders was studied by SEM and TEM for milling times of 85, 110, and 190 min.

3. Results

In Table 1 the phase compositions, the Zr content, and the surface area of the original samples and the milled samples are listed.

The preliminary experiments yielded the following results:

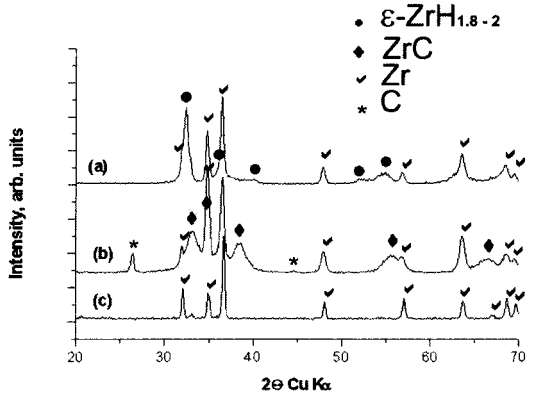

Figure 1. XRD patterns of (a) pure Zr mechanically activated for 15 min in a H_2 flow, (b) Zr−C mechanically activated for 120 min in a He flow, and (c) original Zr.

Mechanical activation of pure graphite in H_2 flow for 120 min gave a highly dispersed graphite powder. The specific surface area *S* of the sample increased from $S = 2$ m^2/g to $S = 175$ m^2/g. The hydrogen sorption was found to be $\sim 2.6 \times 10^{21}$ molecules of H_2/g C, or ~3 monolayers.

Mechanical activation of pure zirconium in H_2 flow resulted in the formation of zirconium hydride. According to TPR data, ~50% of the Zr was transformed to zirconium hydride after 15 min of milling. The XRD results in Figure 1a show that the tetragonal phase ϵ-$ZrH_{1.8-2}$ is the major hydride phase. The lattice constants of this phase were determined as $a = 0.352$ nm, $c = 0.452$ nm, $c/a = 1.284$, while the lattice constants of pure ϵ-$ZrH_{1.8}$ are $a = 0.3492$ nm, $c = 0.4506$ nm, $c/a = 1.290$ (JCPDS 36-1340), and those of ϵ-ZrH_2 are $a = 0.35204$ nm, $c = 0.44504$ nm, $c/a = 1.264$ (JCPDS 17-314). The reaction product ϵ-$ZrH_{1.8-2}$ has an intermediate aspect ratio $c/a = 1.284$, which, however, is closer to that of ϵ-$ZrH_{1.8}$. The specific surface area $S = 0.4$ m^2/g did not change during mechanical treatment.

A zirconium−graphite mixture containing $\sim 1 \times 10^{22}$ atoms of Zr and 1.45×10^{22} atoms of C was mechanically activated in a He flow for 120 min. After the treatment, the powder was partially transformed to cubic ZrC (see Figure 1b), the lattice constant $a = 0.4693$ nm of which is in good agreement with that of pure ZrC (JCPDS 36-1340). According to TPR data, ~25% of the Zr did not transform. The specific surface area *S* of the sample increased from $S = 2$ m^2/g to $S = 8$ m^2/g.

The mechanical activation of zirconium−graphite mixtures in H_2 flow yielded the following results:

Structural changes of the powder were tested after 15, 60, 85, 110, and 190 min of mechanical treatment (see Table 1). Figure 2 shows the XRD spectra of the original Zr (Figure 2a), and of the samples after 15 (Figure 2b), 60 (Figure 2c), and 85 min (Figure 2d) of milling. After 15 min, the powder consists of ϵ-$ZrH_{1.8-2}$, pure Zr, and graphite. The lattice constants of the hydride phase were estimated as $a = 0.351$ nm, $c = 0.448$ nm, $c/a = 1.276$. The α-Zr lattice constants can't be determined because of diffraction peak overlap. According to TPR data, the sample contains ~20% of residual Zr. The BET surface area of this sample is $S = 8.7$ m^2g. Figure 2c shows that after 60 min, the powder consists of ϵ-$ZrH_{1.8-2}$ and graphite, although, according to TPR data, the sample still contains ~2% of Zr. The lattice constants of the hydride phase were determined as $a = 0.351$ nm, $c = 0.448$ nm, $c/a = 1.276$. The BET surface area of this sample is $S = 25$ m^2g. After 85 min of milling, only ϵ-$ZrH_{1.8-2}$ peaks with lattice constants $a = 0.350$ nm and $c = 0.450$ nm, $c/a = 1.285$, are present in the XRD data. The

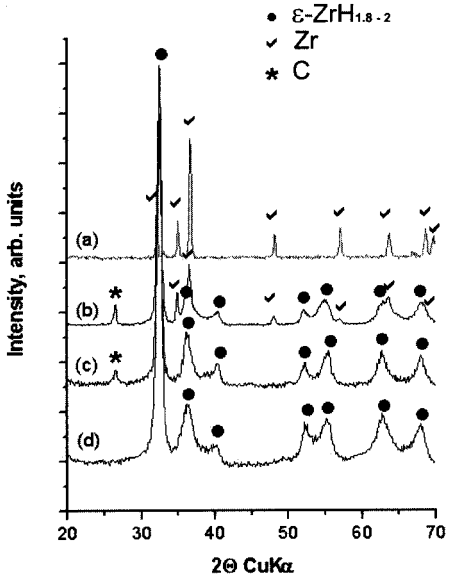

Figure 2. XRD patterns of the original Zr and of the Zr−C powders after different milling times: (a) α-Zr; (b) 15 min; (c) 60 min; (d) 85 min.

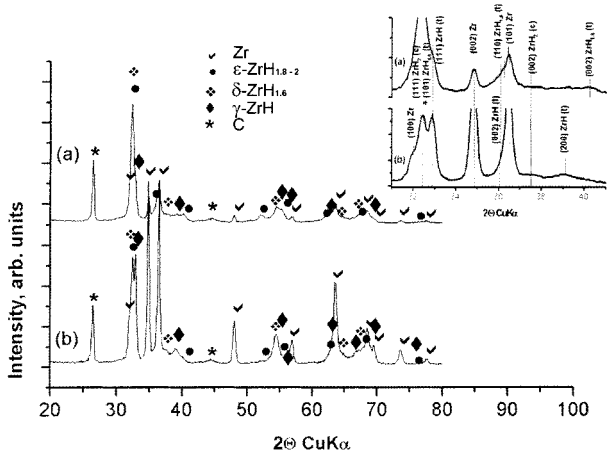

Figure 3. XRD patterns of the Zr−C powders after different milling times: (a) 110 min; (b) 190 min.

XRD peaks of graphite disappear, indicating the amorphization of the carbon. The BET surface area of this sample is $S = 58.4$ m^2/g.

Figure 3 shows XRD patterns of the powders after 110 min (Figure 3a) and 190 min (Figure 3b) of milling. The inset shows the $2\Theta = (31-41)°$ region, which allows an analysis of the phase composition. Besides α-Zr and graphite, one can distinguish three hydride phases: the metastable phase γ-ZrH (JCPDS 2-862), cubic δ-$ZrH_{1.6}$ (JCPDS 34-649), and tetragonal ϵ-$ZrH_{1.8-2}$. The diffraction peaks of α-Zr, γ-ZrH, and δ-$ZrH_{1.6}$ appear, while the intensities of the ϵ-$ZrH_{1.8-2}$ peaks decrease. According to TPR tests, after 110 and 190 min of milling, the powders contain ∼20% and ∼80% of pure zirconium, respectively. The intensity ratio $I(002)/I(101)$ of the newly formed α-Zr has significantly increased, as compared to $I(002)/I(101)$ of the original Zr (see Figures 2a and 3b). The BET surface area decreases to $S = 1.85$ m^2/g after 110 min, and $S < 0.3$ m^2/g after 190 min of milling.

Figure 4 shows SEM micrographs of the original Zr powder (Figure 4a), and after 85, 110, and 190 min of milling. The as-received Zr powder consists of particles with an average size of ∼50 μm and fairly smooth surfaces. Figure 4b shows the morphology of the powder milled for 85 min. The powder

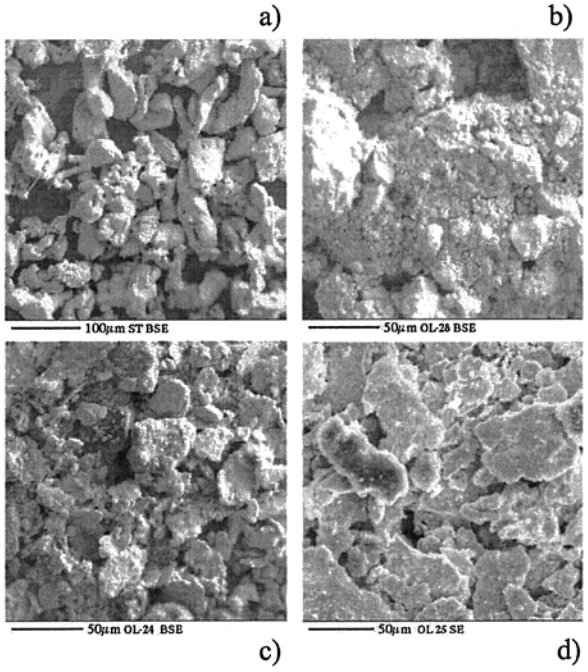

Figure 4. SEM micrographs of the morphology of the powders after different milling times: (a) original Zr; (b) 85 min; (c) 110 min; (d) 190 min.

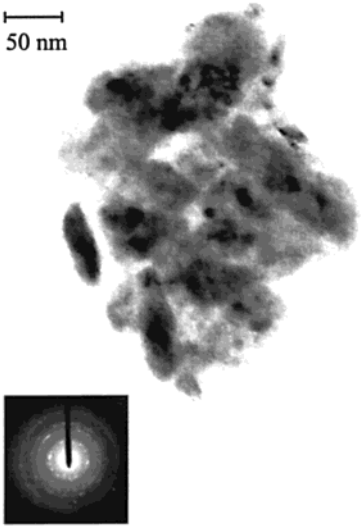

Figure 5. TEM micrograph and corresponding diffraction pattern of 85-min milled Zr−graphite powder.

consists mainly of nanosized small particles lumped together, and a few bigger ones. The average particle size can be estimated as less than 300 nm. After 110 min of milling (see Figure 4c), the powder again consists of larger particles, with a size of ∼50 μm and a flakelike morphology, and some amount of particles as small as ∼300 nm. After 190 min of milling (see Figure 4d), the powder consists mainly of large, flakelike particles, with very few of the small ones.

Figure 5 shows a TEM bright field image and the corresponding diffraction pattern of the powder milled for 85 min. The powder consists of particles with a diameter of about 250 nm. The particles contain small Zr−hydride fragments exhibiting a dark contrast. These fragments are randomly distributed in a matrix of amorphous carbon. Some of the fragments are isolated in the carbon, having fragment sizes down to 3 nm, others form agglomerations of fragments of more or less oblong shape about

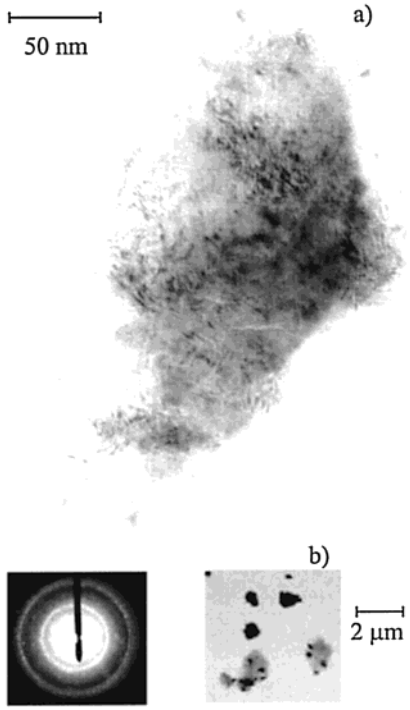

Figure 6. TEM micrograph and corresponding diffraction pattern of 110-min milled Zr−graphite powder.

20 nm × 50 nm in projection. In the TEM micrograph (Figure 6), the microstructure of the powder milled for 110 min can be seen. Figure 6b shows an overview. The particles have sizes up to several micrometers. Some are compact and metallic, as indicated by the dark contrast, others are agglomerations of smaller particles in a carbon matrix. Figure 6a shows a particle with the corresponding diffraction image. It has a highly disordered microstructure. Thin layers (2−8 nm in width) of carbon and Zr-containing phases are intermixed. Separate fragments (about 2−15 nm in size) of Zr-containing phase randomly distributed also exist. The particle exhibits heavy strain contrast. Although such particles are quite typical for the powder tested, other Zr or Zr−hydride particles have macroscopic dimensions (see Figure 6b). Figure 7 shows a TEM bright field image and the corresponding diffraction pattern of the powder milled for 190 min. Zr-containing fragments are embedded in a matrix of carbon. These fragments are bimodal in size, some being compact and facetted with diameters of several 100 nm, others being agglomerations of small fragments, as in Figures 5 and 6. Both the compact particles and the agglomerations are embedded in carbon, which now contains a high amount of partially crystallized nanotubes and whiskers. As for the powder milled for 110 min, an overview micrograph (not shown) shows many micron-sized compact metallic particles too compact for TEM.

Reflection Fourier transform infrared spectroscopy (FTIR) data show valence vibration bands of CH_2 or CH groups formed after decomposition of ϵ-$ZrH_{1.8-2}$, giving evidence that the hydrogen does not evolve into the gas phase but forms hydrocarbons on the surface of carbon particles. This result is from further work in progress and shall be presented in detail in a future publication.

4. Discussion

The most striking feature of the process observed in this study is that in the presence of carbon, the decomposition of ϵ-$ZrH_{1.8-2}$ takes place in permanent hydrogen flow in the second step of transformation.

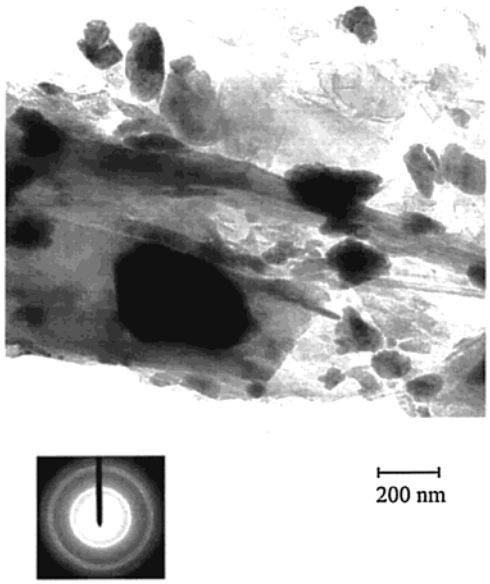

Figure 7. TEM micrograph and corresponding diffraction pattern of 190-min milled Zr−graphite powder.

In the first step, during the first 85 min of milling, a tetragonal zirconium hydride is formed. The aspect ratio c/a of this hydride can be compared to that of ϵ-$ZrH_{1.8}$ ($c/a = 1.290$) and that of ϵ-ZrH_2 ($c/a = 1.264$), both of which are representants of the same phase, but with a slightly different H content.[13] The aspect ratio of the hydride found in this study lies between $c/a = 1.276$ for $t \leq 60$ min and $c/a = 1.285$ for $t = 85$ min. This leads to the assumption that the hydrogen content in the hydride lies between 1.8 and 2 H/Zr, so we call it $ZrH_{1.8-2}$. The hydrogen content in the hydride seems to decrease after 60 min of milling, as the aspect ratio rises. At the same time, the specific surface area and the content of pure Zr in the powder decrease: the BET surface area rises from 0.4 m^2/g for the initial Zr to 58.4 m^2/g after 85 min of milling; the Zr content is nearly zero after these 85 min, according to TPR data. A look at the preliminary experiments shows that the carbon plays a vital role in this process: after 15 min of milling in hydrogen flow without carbon, about 50% of pure Zr transformed to hydride but did not change its specific surface area, whereas after the same treatment but in the presence of carbon, about 80% of the Zr transformed to hydride and enlarged its surface area noticeably. In contrast, the milling of pure carbon in hydrogen flow for 120 min results in a sharp increase of the specific surface area of the residual carbon from 2 to 175 m^2/g, and the milling of a Zr−C mixture in helium flow for 120 min results in rather sluggish carbide formation accompanied by a moderate increase in specific surface area (all results are listed in Table 1).

Figure 8(i) shows the H_2 sorption on the Zr−C and C powders under flow milling conditions, and Figure 8(ii) shows the variations of both Zr content (detected by TPR) and BET surface area for Zr−C powders after different milling times. For the first stage process, only milling times up to 85 min are relevant. The Zr−C powder (curve 8(i)a) exhibits a high sorption rate during the first 15−20 min of the treatment. Then the H_2 sorption rate decreases by a factor of 5−6 and becomes comparable with that on pure C (curve 8(i)b). Thus, at the beginning of the milling process, most of the hydrogen reacts with Zr, forming ϵ-$ZrH_{1.8-2}$. At the same time, the content of pure Zr decreases and the specific surface area increases. Obviously, as the zirconium takes on hydrogen and reacts to hydride, the hydride becomes more and more brittle, thus

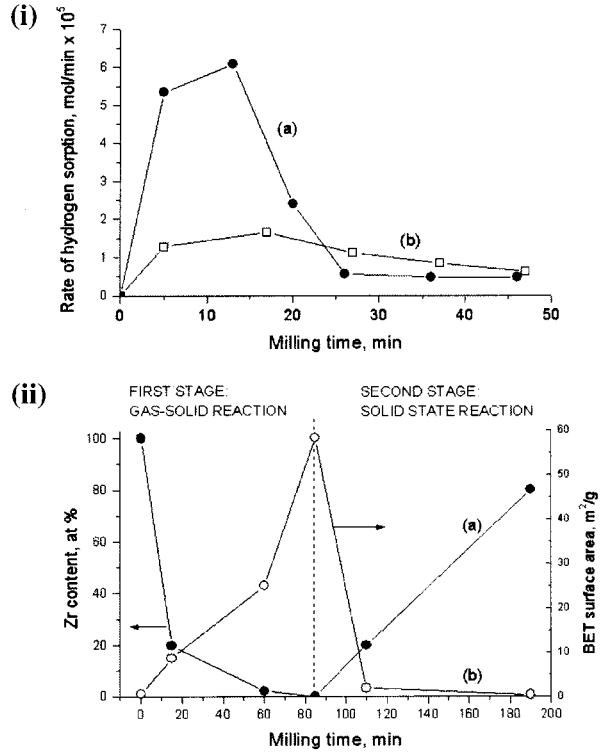

Figure 8. (i) Kinetic curves of hydrogen sorption on (a) Zr−C mixture (1.5 g of Zr + 0.3 g of C) and on (b) graphite (1.8 g) measured during the mechanical activation in H_2 flow. (ii) Variations of (a) Zr content and (b) BET surface area for Zr−graphite powders after different milling times.

literally falling to pieces, which are only a few nm in size after 85 min of milling, see Figure 5. The transformation of Zr to Zr−hydride is likely to be controlled by the rate of creating fresh surfaces accessible for H_2, i.e. by the rate of reducing the powder size. At the same time, the specific surface area of the carbon rises too, as it does when carbon alone is milled in H_2 flow. According to Chen and co-workers,[14] graphite with a high surface area has a large internal surface due to nanosized pores. These pores can't be seen in TEM micrographs because of the poor contrast of carbon, but a high carbon surface area due to pores seems likely, since the individual powder particles are rather large, i.e. of the order of several 100 nm. Highly dispersed nanoporous graphite powder seems to provide access of H_2 to Zr particles, which after hydride formation, under prolonged milling, disintegrate into nanosized particles that are now covered by carbon and agglomerate to particles, as shown in Figure 5. It has to be stressed that during the described process, the graphite becomes amorphous with quasicrystalline layers wrapping the hydride nanoparticles.

The solid-state transformation ϵ-$ZrH_{1.8-2}$ + am.C → δ-$ZrH_{1.6}$ + hydrocarbon → γ-ZrH + hydrocarbon → α-Zr(C) + hydrocarbon is the major reaction of the second stage. Once started, it was found to take place under the milling in H_2 flow: the powder milled for 110 min contains ∼20 at. % of Zr, the powder milled for 190 min contains ∼80 at. % of Zr, whereas after 85 min of milling, virtually no pure Zr was detectable at all. The reaction products δ-$ZrH_{1.6}$, γ-ZrH, and α-Zr(C) are detected simultaneously after 110 and 190 min of milling, although the steps of the reaction occur in succession. The reason for this is most probably that individual particles are in different stages of the reaction, presumably because of different particle sizes. The released hydrogen seems to form cyclic hydrocarbons on the surface of the carbon, as reflection Fourier transform infrared spectroscopy (FTIR) data show valence vibration bands of CH_2 or CH groups. Further investigations are in progress to establish the nature of these hydrocarbons.

Decomposition of metal hydrides initiated by mechanical treatment is well-known. The transformation of $PdH_{0.7}$ to $PdH_{0.01}$ + Pd in response to the shear deformation under high pressure is described by Teplov and co-workers.[15] In a previous work by our group,[6] it was found that ϵ-ZrH_2 lost ∼50% of its hydrogen during milling for 180 min in He flow: the hydrogen atoms diffused from the bulk to the surface of the sample and then evolved to the gas phase after recombination to H_2. It was further found[6] that the decomposition of ϵ-ZrH_2 in a CO or a CO_2 flow was caused by both mechanical deformation and by insertion of C and O atoms into the ϵ-ZrH_2 bulk.

The carbon seems to stimulate the decomposition of $ZrH_{1.8-2}$, as the decomposition of the hydride is much faster in the presence of carbon, even under persisting hydrogen flow, than the decomposition of the hydride alone under helium flow.[6] A slight increase in the lattice constants of α-Zr, product of ϵ-$ZrH_{1.8-2}$ decomposition, as compared to bulk values, is an evidence for the introduction of carbon atoms into the zirconium. The hydrogen atoms may be displaced from the tetrahedral positions in the ϵ-$ZrH_{1.8-2}$ lattice by interstitial carbon atoms, if they occupy the neighboring octahedral positions.[10] A high concentration of structural defects caused by the mechanical treatment can raise the solubility of C in α-Zr, which is quite low under thermal and mechanical equilibrium. This metastable carbon solution can suppress carbide formation. From the point of view of thermodynamics, the formation of a Zr−C solid solution under decomposition of the Zr−hydride is not surprising: the affinity of Zr to C is higher than to H, as indicated by the heats of formation of ZrH_2, $H(298) = -56\,484$ J/g-atom[16] and ZrC, $H(298) = -103\,554$ J/g-atom.[16] So the reaction of Zr with C is energetically more favorable than the reaction with hydrogen. On the other hand, the mobility of hydrogen is much higher than that of carbon. At the beginning of the milling, the hydrogen is in the gas phase and can form the hydride at once, while the carbon, being present as graphite, cannot react with the zirconium immediately. Thus we observe the formation of ϵ-$ZrH_{1.8-2}$ in the first 85 min of milling, accompanied by a dramatic decrease in particle size as well as the amorphization of the carbon. After prolonged milling, the carbon is amorphous and the individual carbon atom less tightly bonded than in graphite; the extremely small zirconium particles offer a high specific surface area and thus access for the carbon atoms. A high density of structural defects makes the metastable solution of carbon possible because of the higher affinity of zirconium to carbon as compared to hydrogen.

The newly formed Zr(C) particles are again micron-sized, as the initial Zr powder, but the morphology of the particles has changed from roundish to flake-like with a (001) habit plane, as indicated by the high intensity of the (001) X-ray reflections. Particles of newly formed pure Zr, not as brittle as the hydride, are friction welded by prolonged milling. These particles are deformed parallel to (001), since this is the major slip system in hexagonal metals.

5. Conclusions

Mechanical activation of the Zr−graphite mixture in the hydrogen flow was described as a two-stage process. Each stage was dealt in a framework of chemical transformations and morphological transformations. The first stage is characterized by the formation of a highly dispersed composite material,

whose particles contain ϵ-$ZrH_{1.8-2}$ fragments of several nm in size embedded in an amorphous carbon matrix. In terms of chemical transformations, the first stage is characterized by the formation of ϵ-$ZrH_{1.8-2}$ from Zr metal through a gas−solid reaction: α-Zr + $H_2 \rightarrow \epsilon$-$ZrH_{1.8-2}$.

The second stage is characterized by the formation of micron-sized plate-like particles containing Zr fragments embedded in partly crystalline carbon layers as well as micron-sized metallic Zr plates. In a framework of the chemical transformations, the second stage is characterized by the decomposition of ϵ-$ZrH_{1.8-2}$ through a solid-state reaction: ϵ-$ZrH_{1.8-2}$ + am.C $\rightarrow$ δ-$ZrH_{1.6}$ + hydrocarbon $\rightarrow$ γ-ZrH + hydrocarbon $\rightarrow$ Zr(C) + hydrocarbon. Further investigations will establish the nature of these hydrocarbonss formed during the transformation process.

Acknowledgment. We are thankful to Prof. P. Yu. Butyagin, Dr. A. N. Streletskii (Institute of Chemical Physics RAS), and Dr. A. Pundt (Institute of Materials Physics of the University of Göttingen) for valuable comments and discussion, to Dr. T. I. Khomenko (Institute of Chemical Physics RAS) for performing TPR experiments, and to Dr. H. Jander (Institute of Physical Chemistry of the University of Göttingen) for the preparation of TEM samples. This work is supported in part by Ministry of Education, Science, and Culture of Japan (C), No. 12650692, and by the Russian Foundation for Basic Research, Project No. 01-03-32803.

References and Notes

(1) Calka, A.; Nikolov, J. I.; Ninham, B. W. *Proceedings of the 2nd International Conference on Structural Application of Mechanical Alloying,* Vancouver, Canada; 1993; p 189.

(2) Memezawa, A.; Aoki, K.; Masumoto, T. *Mater. Sci. Eng. A* **1994**, *181/182,* 1263.

(3) Calka, A. *Appl. Phys. Lett.* **1991**, *89,* 1568.

(4) Streletskii, A. N.; Morozova, O. S.; Berestetskaya, I. V.; Borunova, A. B. *Mater. Sci. Forum* **1998**, *269−272,* 283.

(5) Streletskii, A. N.; Morozova, O. S.; Berestetskaya, I. V.; Borunova, A. B.; Butyagin, P. Yu. *Mater. Sci. Forum* **1996**, *225−227,* 539.

(6) Streletskii, A. N.; Morozova, O. S.; Berestetskaya, I. V.; Borunova, A. B.; Leonov, A. V.; Kryukova, G. N. *J. Metastable Nanocryst. Mater.* **2000**, *8,* 429.

(7) P. Yu. Butyagin, Streletskii, A. N. Morozova, O. S.; Leonov, A. V.; Berestetskaya, I. V.; Borunova, A. B. *Chem. Phys. Rep.* **1998**, *17,* 521.

(8) Beck, R. L. *Trans. ASM* **1962**, *55,* 52.

(9) Maccay, K. M.; *Hydrogen Compounds of the Metallic Elements*; E. & G. N. Spon LTD: London, 1966.

(10) Andrievskii, R. A.; Umanskii, Ya. S. *Interstitial Phases*; Nauka: Moscow, 1977 (in Russian).

(11) Butyagin, P. Y. Streletskii, A. N.; Morozova, O. S.; Berestetskaya, I. V.; Borunova, A. B. *Dokl. Phys. Chem.* **1994**, *336,* 105.

(12) Mirkin, A. I. *Handbook on X-ray Diffraction Analysis of Polycrystals*; Nauka: Moscow, 1961 (in Russian).

(13) Morozova, O. S.; Leonov, A. V.; Khomenko, T. I.; Korchak, V. N. *Metastable, J. Nanocryst. Mater.* **2001**, *10,* 415.

(14) Chen, Y.; Fitz Gerald, J.; Chadderton, L. T.; Chaffron, L. *J. Metastable Nanocryst. Mater.* **1999**, *2−6,* 375.

(15) Teplov, V. A.; Pilyugin, V. P.; Gaviko, V. S.; Shchegoleva, N. N.; Gervas'eva, I. V.; Patselov, A. M. *Phys. Met. Metallogr.* **1997**, *84,* 525.

(16) Knacke, O.; Kubaschewski, O.; Hesselmann, K. *Thermochemical Properties of Anorganic Substances*; Springer: Berlin, 1991.